DOI: 10.3901/CJME.2015.0307.025, available online at www.springerlink.com; www.cjmenet.com; www.cjme.com.cn

Planetary Gear Profile Modification Design Based on Load Sharing Modelling

IGLESIAS Miguel, FERNÁNDEZ DEL RINCÓN Alfonso, DE-JUAN Ana Magdalena, GARCIA Pablo, DIEZ Alberto, and VIADERO Fernando*

Mechanical Engineering Research Group, University of Cantabria, Santander 39005, Spain

Received February 11, 2015; revised March 3, 2015; accepted March 7, 2015

Abstract: In order to satisfy the increasing demand on high performance planetary transmissions, an important line of research is focused on the understanding of some of the underlying phenomena involved in this mechanical system. Through the development of models capable of reproduce the system behavior, research in this area contributes to improve gear transmission insight, helping developing better maintenance practices and more efficient design processes. A planetary gear model used for the design of profile modifications ratio based on the levelling of the load sharing ratio is presented. The gear profile geometry definition, following a vectorial approach that mimics the real cutting process of gears, is thoroughly described. Teeth undercutting and hypotrochoid definition are implicitly considered, and a procedure for the incorporation of a rounding arc at the tooth tip in order to deal with corner contacts is described. A procedure for the modeling of profile deviations is presented, which can be used for the introduction of both manufacturing errors and designed profile modifications. An easy and flexible implementation of the profile deviation within the planetary model is accomplished based on the geometric overlapping. The contact force calculation and dynamic implementation used in the model are also introduced, and parameters from a real transmission for agricultural applications are presented for the application example. A set of reliefs is designed based on the levelling of the load sharing ratio for the example transmission, and finally some other important dynamic factors of the transmission are analyzed to assess the changes in the dynamic behavior with respect to the non-modified case. Thus, the main innovative aspect of the proposed planetary transmission model is the capacity of providing a simulated load sharing ratio which serves as design variable for the calculation of the tooth profile modifications.

Keywords: transmission, planetary gear, load sharing, relief, profile modification

1 Introduction

Planetary gears are used to transmit power in numerous industrial applications, being the most compact and lightest possible drives[1], but even so they are progressively subjected to higher requirements of torque, speed and compactness. In order to satisfy these demands, researchers try to improve their understanding of the underlying phenomena involved in planetary gear power transmission, through the development of models capable of realistically reproduce the system behavior. Research in this area contributes to improve gear transmission insight, helping developing better maintenance practices[2] and more efficient design processes.

As it has been pointed out, one of the main advantages of planetary gearing is the compactness. For high torques, instead of using large wheels, a simpler solution consists in splitting the load into a number of paths, so that loadings per unit facewidth for a given wheel size remain below nominal values, while the torque is multiplied. Ideally, each path should carry the same load. However, real planetary gear transmissions present manufacturing deviations and variable stiffness, which lead to a different load sharing ratio(LSR) for each path. This causes dynamic problems, higher loads and reliability concerns, due to the fact that the nominal load per teeth width may be surpassed. The LSR has been previously studied from both experimental[3–4] and computational modeling approaches. This last approach includes models that range from simple analytical[5] to complex hybrid models, combining analytical and finite element studies[6]. One of the main sources of uneven LSR, apart from the manufacturing errors in the system, is the existence of "out of line of action" (OLOA) contacts, for example at the tip of the teeth, where the involute profile ends and the teeth pairs come into contact in advance. In order to avoid this problem, modified profiles are of common use in the gear industry.

Some studies have been done in profile modification in planetary transmissions, first addressed by PALMER and FUERHER[7], where an improvement in the noise generation of a planetary transmission was demonstrated with the introduction of profile modifications.

* Corresponding author. E-mail: viaderof@unican.es
Supported by the Project DPI2013-44860 funded by the Spanish Ministry of Science and Technology

Regarding planetary modeling including profile deviations several works have been presented[8–10], extracting a variety of conclusions, like the diminishing of some of the mesh forces harmonics, or the reduction of the orbit radii for central elements. A more specific study on profile modification effects on the overall planetary gear dynamics was performed by BAHK and PARKER[11]. Using perturbation methods, they found that the dynamic analysis at a whole system level is necessary for the design of tooth modifications with the goal of planetary gear vibration reduction. This last conclusion comes to justify the complete model of planetary transmission that is used in this work for the profile modification design.

Due to its spatial configuration, planetary transmissions are difficult to model. The static transmission error has been used as excitation to model planetary transmissions[12–13], but recent studies point that this approach, while remaining relatively valid for ordinary transmissions, may not be applicable to multi-mesh transmissions such as planetary ones[14]. Enhanced models including time-varying stiffness give better off-resonance responses, and are also used to identify regions of resonance, where damping and other nonlinear phenomena strongly affect the behavior[15–16]. The latest and more advanced planetary transmission models are those based on computational approaches, frequently including FEM techniques in combination with different contact models[17], in some cases even considering completely flexible bodies during the dynamic simulations[8].

In this work, a planetary transmission model developed by the authors and based on a previous mesh model[18–19] is applied to the design of profile modifications in a planetary transmission. The geometry definition aspects of the model are described with great detail, focusing the description on the inner gear, being the approach completely analogous for the external gear wheels. With the method implemented, aspects such as the undercutting of the teeth and the hypotrochoid section definition are implicitly taken into account. The introduction of a rounding arc at the tip of the teeth is justified and explained. A procedure for the modeling of profile deviations is then presented, with the possibility of linear and parabolic modification, and any size and length of both tip and bottom relief. Regarding the contact force calculation and the dynamic implementation, a summary of the procedure is presented, referencing those works in which further descriptions can be found. An analytical formulation for the contact problem is hybridized with finite element models in order to compute the contact forces[18].

Finally, a real planetary transmission is used as application example. The design of a set of profile modifications is done based on the improvement of the load sharing characteristic up to a certain point, and then the two versions of the transmission(modified and not modified) are modeled and their dynamic behavior simulated, assessed and compared.

2 Planetary Gear Basic Geometry

The first problem to be addressed when building a planetary gear transmission is the appropriate description of the wheels geometry. This definition should be consistent enough to represent with flexibility and robustness the widest possible range of parametric variations of the transmission.

This section describes the different phases of the profile definition, without taking into account the profile modifications, which will be introduced and described later on. For the sake of simplicity and shortness, the procedure will be described in detail, but limited to the inner gear profile definition. For external gears the procedure is completely analogous, and can be found thoroughly described in[20].

In this model the generation of the gear profile is done by mathematically mimicking the real cutting process, using the vector approach proposed by LITVIN, et al[21]. This procedure provides a high degree of realism, and in addition it provides great versatility. It allows for the generation of shifted gears, and also take into account implicitly issues such as undercutting and trochoid definition. In order to avoid the singularity of corner contacts, a rounding arc is added at the tip of the teeth, according to VEDMAR[22] approach.

2.1 Cutting tools

For the modeling of a planetary transmission both internal and external gear are required. For the latter (sun and planet gears) it is used a normalized rack cutter, while for the inner ring gear profile definition a pinion shaper cutter has been adopted.

In Fig. 1 a single tooth of the shaper cutter tool is shown. Each section of the tool is parameterized, allowing for an easy definition of the same. Three sections of interest are found: two corresponding to the outer and inner arcs of head and bottom circumferences, and another one corresponding to the involute tooth flank of the tool.

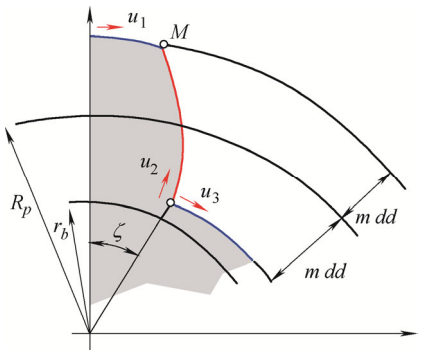

Fig. 1. Cutting tool parameterization

Once the tool is completely defined, it is also necessary to define a set of coordinate systems as shown in Fig. 2,

that will be used for the analytical cutting process. The other parameters that define the tool are the m module, the addendum coefficient ad, dedendum coefficient dd and primitive and base radii R_P and r_b. The module is expressed in milimeters, and the addendum, dedendum and shifted factor x are normalized by the module. Next, each section of the pinion shaper are defined within the pinion system of reference.

$$\boldsymbol{r}_1^{\text{tool}}(u_1,v_1)=\begin{pmatrix}(R_P+m\,ad)\sin u_1\\(R_P+m\,ad)\cos u_1\\v_1\end{pmatrix},\quad 0\leqslant u_1\leqslant u_{1\max}, \tag{1}$$

$$\boldsymbol{r}_2^{\text{tool}}(u_2,v_2)=\begin{pmatrix}\dfrac{r_b}{\cos u_2}\sin(\zeta-\tan u_2+u_2)\\\dfrac{r_b}{\cos u_2}\cos(\zeta-\tan u_2+u_2)\\v_2\end{pmatrix}, \tag{2}$$

$$\arccos\left(\frac{r_b}{R_p-m\,dd}\right)\leqslant u_2\leqslant\arccos\left(\frac{r_b}{R_p+m\,dd}\right),$$

$$\boldsymbol{r}_3^{\text{tool}}(u_3,v_3)=\begin{pmatrix}(R_P+m\,dd)\sin u_3\\(R_P+m\,dd)\cos u_3\\v_3\end{pmatrix}, \tag{3}$$

$$u_{3\min}\leqslant u_3\leqslant\frac{\pi}{z}.$$

Parameters u_i and v_i determine the position of a point along each of the sections considered in the shaper. The parameter u_i provides variation within the plane perpendicular to the gear axis, and the parameter v_i varies between $-b/2$ and $b/2$, being b the pinion width in milimeters. The limits for the variation of u_1 and u_3 are defined by the following expressions:

$$u_{1\max}=\frac{\pi}{2z}+Ev\left[\arccos\left(\frac{r_b}{R_P}\right)\right]-Ev\left[\arccos\left(\frac{r_b}{R_P+m\,ad}\right)\right], \tag{4}$$

$$u_{1\min}=\frac{\pi}{2z}+Ev\left[\arccos\left(\frac{r_b}{R_P}\right)\right], \tag{5}$$

where the well-known involute function is $Ev(\varphi)=\tan(\varphi)-\varphi$.

2.2 Envelope and meshing condition

In the manufacture of gears by shaper, the material is removed from the wheel up to a certain limit, which is defined by the envelope of the tool profile with respect to the manufactured gear. The analytical process is completely equivalent, being necessary to find the envelope to a family of curves. Applying the classical approach of differential geometry a necessary condition for the existence of this envelope can be obtained. If this condition is simplified exploiting the properties of the relative velocity between profiles, it results in the following meshing condition[21]:

$$\boldsymbol{n}^S_{\text{profile}}\bullet\boldsymbol{v}^S_{\text{relative}}=0. \tag{6}$$

Once satisfied, this equation indicates which points in the profile of the tool have a relative velocity tangential to the surface, and are therefore likely to be cutting for a certain position.

In the particular case of internal gear cutting, the relative motion of the shaper with respect to the ring gear is given by the pure rolling of the polar curve associated with the shaper on the polar curve associated with the ring. Thus, these two curves can be defined as the pitch circles for pinion and ring, of radii R_P and R_R. The motion is described in Fig. 2, where the three reference systems used are noticeable: one associated with the ring gear(in red), one with the pinion cutter shaper(in blue) and the global reference system(in black). During the cutting process the tool can undergo a deliberate shift in its position, which is defined by the parameter x(shift factor), allowing for the generation of shifted gears, with non-normalized tooth widths.

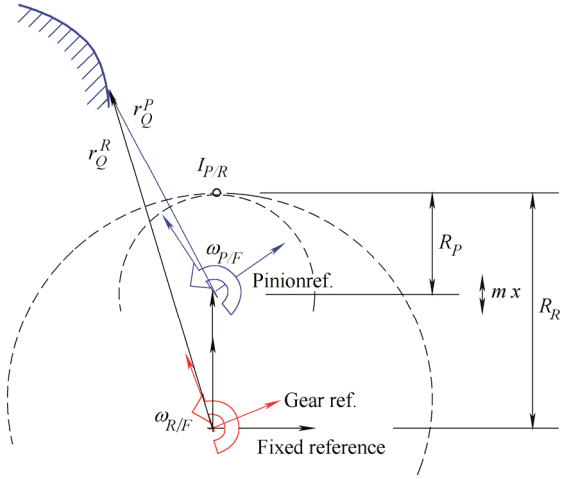

Fig. 2. Cutting process and reference systems

The relative movement between the shaper and the ring will be characterized by their corresponding axodes. Hence, it is possible to obtain the relative velocity of any point Q at the tool profile by

$$\boldsymbol{v}^F_{Q(R/F)}=\boldsymbol{v}^F_{Q(R/P)}+\boldsymbol{v}^F_{Q(P/F)}\rightarrow\boldsymbol{v}^F_{Q(R/P)}=\boldsymbol{v}^F_{Q(R/F)}-\boldsymbol{v}^F_{Q(P/F)}, \tag{7}$$

which is a vectorial equation expressing the velocity of the point Q at the ring(R) in the movement with respect to the pinion(P), expressed in the global reference system(F). Taking into account that the motion of Q is a rotation for any given relative motion, and knowing the distance between the centers of the wheels, from Eq. (7) it can be

obtained:

$$\boldsymbol{v}_{Q(R/P)}^{F}=\dot{\theta}_R\begin{Bmatrix}\left(1-\dfrac{z_R}{z_P}\right)\left[r_x^P\sin\left(-\theta_P\right)-r_y^P\cos\theta_P\right]+d\\ \left(1-\dfrac{z_R}{z_P}\right)\left[r_x^P\cos\theta_P-r_y^P\sin\left(-\theta_P\right)\right]\\ 0\end{Bmatrix}. \quad (8)$$

Thus only remains to calculate the normal to the tool profiles to raise the meshing condition Eq. (6). For curves defined parametrically, the normal is

$$\boldsymbol{n}_{\text{profile}}^{\text{tool}}=\boldsymbol{t}\times\boldsymbol{k}=\frac{d\boldsymbol{n}_{\text{profile}}^{\text{tool}}(u)}{\mathrm{d}u}\times\boldsymbol{k}. \quad (9)$$

By applying this expression to each of the sections defined of the tool profile it is possible to obtain the corresponding normal to each section. Then, a change in the reference system must be applied, to have all vectors defined in the global reference. Thus,

$$\begin{aligned}\boldsymbol{n}_1^F&=\begin{Bmatrix}-\sin\left(u_1-\theta_P\right)\\ -\cos\left(u_1-\theta_P\right)\\ 0\end{Bmatrix},\\ \boldsymbol{n}_2^F&=\begin{Bmatrix}\cos\left(\tan u_2-\zeta+\theta_P\right)\\ \sin\left(\tan u_2-\zeta+\theta_P\right)\\ 0\end{Bmatrix},\\ \boldsymbol{n}_3^F&=\begin{Bmatrix}-\sin\left(u_3-\theta_P\right)\\ -\cos\left(u_3-\theta_P\right)\\ 0\end{Bmatrix}.\end{aligned} \quad (10)$$

Finally, Eq. (6) can be particularized for each of the cutter sections, substituting Eqs. (8) and (10). The meshing condition for each section, which link the parameters u_i with the angular positions of pinion and ring are then obtained:

$$\text{Section } 1\rightarrow d\sin\left(u_1-\theta_P\right)=0; \quad (11)$$

$$\text{Section } 2\rightarrow -r_{\text{b}}\left(1-\frac{z_R}{z_P}\right)+d\cos\left(\tan\left(u_2\right)-\zeta+\theta_P\right)=0; \quad (12)$$

$$\text{Section } 3\rightarrow d\sin\left(u_3-\theta_P\right)=0. \quad (13)$$

2.3 Gear profile

The gear profile is obtained by expressing each of the sections in Eq. (13) in the coordinate system of the ring, simultaneously verifying the meshing condition Eqs. (11)–(13). The coordinate transformation from P to R is done in two phases. The first is a rotation and translation of the reference system of the shaper to the global or fixed coordinate system. The second phase is another rotation to reach the ring reference system. Each of these operations can be expressed by the corresponding homogeneous transformation matrix, as shown below:

$$\boldsymbol{M}_{P\rightarrow F}=\begin{pmatrix}\cos\left(-\theta_P\right)&\sin\left(-\theta_P\right)&0&0\\ -\sin\left(-\theta_P\right)&\cos\left(-\theta_P\right)&0&d\\ 0&0&1&0\\ 0&0&0&1\end{pmatrix}, \quad (14)$$

$$\boldsymbol{M}_{F\rightarrow R}=\begin{pmatrix}\cos\theta_R&\sin\theta_R&0&0\\ -\sin\theta_R&\cos\theta_R&0&0\\ 0&0&1&0\\ 0&0&0&1\end{pmatrix}. \quad (15)$$

Multiplying the matrices in reverse order, the final homogeneous transformation matrix is obtained:

$$\boldsymbol{M}_{P\rightarrow R}=\begin{pmatrix}\cos\left(\theta_R-\theta_P\right)&\sin\left(\theta_R-\theta_P\right)&0&d\sin\left(\theta_R-\theta_P\right)\\ -\sin\left(\theta_R-\theta_P\right)&\cos\left(\theta_R-\theta_P\right)&0&d\cos\left(\theta_R-\theta_P\right)\\ 0&0&1&0\\ 0&0&0&1\end{pmatrix}. \quad (16)$$

This can be applied to each of the sections of the tool defined in Eqs. (1)–(3) providing

$$r_i^R\left(u_i,v_i,\theta_R\right)=\begin{Bmatrix}\cos\left(\theta_R-\theta_P\right)r_{ix}^P+\sin\left(\theta_R-\theta_P\right)r_{iy}^P+d\sin\theta_R\\ -\sin\left(\theta_R-\theta_P\right)r_{ix}^P+\cos\left(\theta_R-\theta_P\right)r_{iy}^P+d\cos\theta_R\\ v_i\end{Bmatrix}. \quad (17)$$

The meshing equations for the first and third section relationships between parameters u_1 and θ_{P} can be obtained, so that substituting in Eq. (17):

$$u_1=\theta_1\Rightarrow \boldsymbol{r}_1^R=\begin{Bmatrix}\left(\dfrac{z_R}{z_P}R_P+m\,ad+m\,x\right)\sin\theta_R\\ \left(\dfrac{z_R}{z_P}R_P+m\,ad+m\,x\right)\cos\theta_R\\ v_1\end{Bmatrix}, \quad (18)$$

$$u_3=\theta_3\Rightarrow \boldsymbol{r}_3^R=\begin{Bmatrix}\left(\dfrac{z_R}{z_P}R_P-m\,ad+m\,x\right)\sin\theta_R\\ \left(\dfrac{z_R}{z_P}R_P-m\,ad+m\,x\right)\cos\theta_R\\ v_3\end{Bmatrix}. \quad (19)$$

It is easy to see that these equations describe the profile of the ring wheel bottom and head circumferences respectively. For the head(or outside circumference) this equation has only some relevance, since the actual manufacturing process involves a ring of material which defines the actual thickness of the gear. From the meshing equation for section 2 the parameter u_2 can be found as a function of θ_R:

$$u_2 = \arctan\left(\arccos\left(\frac{r_b}{d}\left(\frac{z_R}{z_P}-1\right)\right)+\zeta-\frac{z_R}{z_P}\theta_R\right), \tag{20}$$

substituting

$$\boldsymbol{r}_2^R = \begin{pmatrix} \dfrac{r_b}{\cos u_2}\sin\left(\zeta-\tan(u_2)+u_2+\theta_R\left(1-\dfrac{z_R}{z_P}\right)\right)+d\sin\theta_R \\ \dfrac{r_b}{\cos u_2}\cos\left(\zeta-\tan(u_2)+u_2+\theta_R\left(1-\dfrac{z_R}{z_P}\right)\right)+d\cos\theta_R \\ v_2 \end{pmatrix}, \tag{21}$$

This is the involute profile of the inner gear. The section that links the involute profile and the bottom circumference will be cut and defined by the point at the tool designated as M in Fig. 1. This profile section correspond to a hypotrochoid, and for its definition any of the two cutter portions that meet in M can be used, as long as the parameter u is set to coincide with M. In this case, the first section has been used, with u_1 set to its maximum(M).

$$\boldsymbol{r}_{\text{troc}}^R = \begin{pmatrix} (R_P+m\,ad)\sin\left(\theta_R\left(1-\dfrac{z_R}{z_P}\right)+u_{1\max}\right)+d\sin\theta_R \\ (R_P+m\,ad)\cos\left(\theta_R\left(1-\dfrac{z_R}{z_P}\right)+u_{1\max}\right)+d\cos\theta_R \\ v_1 \end{pmatrix}. \tag{22}$$

Thus, they are only left for definition the variation intervals for the parameters u_i and θ_R for which each tool section is actually actively cutting and which not necessarily coincide with those limits established in Eqs. (1) to (5). The next conditions must be observed:

(1) To limit the involute profile, the tool will only cut up to the point where the radii of the points being defined match the external radius of the head circumference. The radius of the involute is given by

$$R_{\text{inv}} = \sqrt{\left(r_{2x}^R\right)^2+\left(r_{2y}^R\right)^2}, \tag{23}$$

and the equation which provides the limit for the parameter variation is then

$$\left(R_{\min}\right)^2-\left(r_{2x}^R\right)^2-\left(r_{2y}^R\right)^2 \rightarrow u_{2\min}, \theta_{R2\min}. \tag{24}$$

(2) For the circumference corresponding with the head of the teeth, which meets the involute section, the limiting equation can be

$$r_{2x\min}^R - r_{3x}^R = 0 \rightarrow \theta_{R3\min}. \tag{25}$$

(3) Finally, for the hypotrochoid section, once fixed the parameter u_1, θ_R will vary between the values for which M is actively cutting, which corresponds to

$$\theta_{R2\min} \leqslant \theta_{R\text{troc}} \leqslant \theta_{R1\min}. \tag{26}$$

Both tool profile and generated inner gear tooth can be seen in Fig. 3.

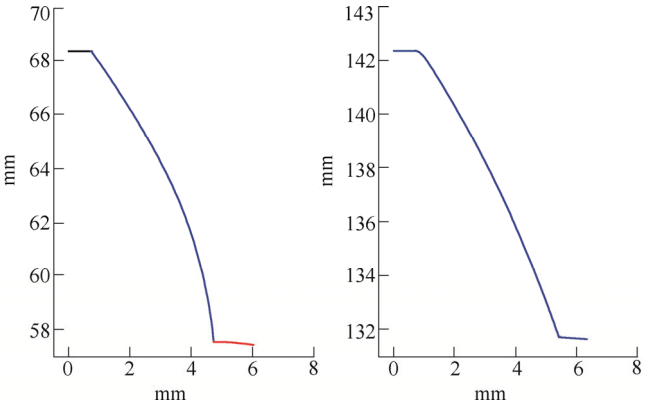

Fig. 3. Tool and generated inner gear tooth profile

2.4 Undercutting

The approach described in the previous subsections also allows for the consideration of undercutting(Fig. 4) during the cutting process, providing for an extra degree of realism to the gear profile definition. When the undercutting occurs at the external gears, the new limits between sections must be numerically determined, as the involute profile is modified by the cutter after its initial definition. This procedure is described in Ref. [20].

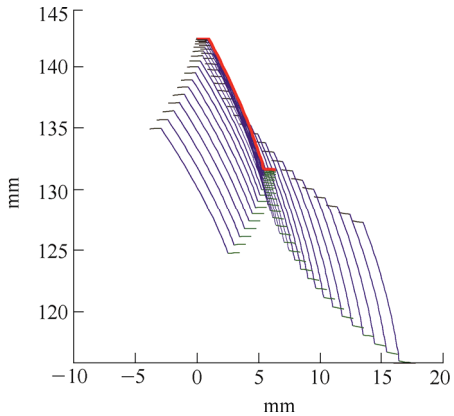

Fig. 4. Inner gear undercutting

In the case of inner gears, where the focus of this section is applied, the undercutting consists on the removal of material from the wheel tooth tip during the extraction of the shaper teeth, due to an excess in the size dimension of both gears. In Fig. 4 this effect is modelized according to the procedure described, where the shaper used presents a number of teeth which exceeds the limit defined by Eq. (27) for which the nonundercutting condition is guaranteed LITVIN[21]:

$$z_P \leqslant z_R - 4.42. \tag{27}$$

For a pressure angle of 30º and considering the axial generation method.

2.5 Teeth tip rounding arc

According to the gear profile definition described above, it can be seen that the intersection of the head circumference and the involute profile results in a sharp edge. Although kinematically speaking this should not be a problem, real gears are flexible, and during the meshing process corner contacts could arise, which would lead to problems in the model contact force calculation. In order to avoid this singularity, a tip rounding (Fig. 5) is added to the tip of the teeth, following VEDMAR[22] approach both in external and internal gears, according to the process described below.

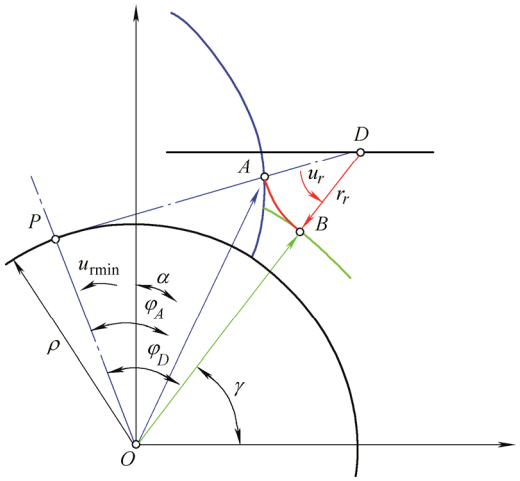

Fig. 5. Graphic construction for the tip rounding definition

A new circular section of the tooth profile is defined as a rounding arc as follows:

$$\boldsymbol{r}_{\text{rou}}^{R} = \begin{pmatrix} D_x - r_{\text{rou}} \cos u_{\text{rou}} \\ D_y - r_{\text{rou}} \sin u_{\text{rou}} \\ v_{\text{rou}} \end{pmatrix}, \quad \varphi_A - \alpha \leqslant u_{\text{rou}} \leqslant \gamma, \tag{28}$$

where

$$D_x = \overline{OD}\cos\gamma, D_y = \overline{OD}\sin\gamma, \tag{29}$$

and

$$\overline{OD} = \overline{OB} + r_{\text{rou}} = R_{\min} + r_{\text{rou}}. \tag{30}$$

Angle γ can be defined according to Fig. 5 as

$$\gamma = \frac{\pi}{2} - \alpha - (\varphi_D - \varphi_A) = \frac{\pi}{2} - \alpha - \arccos\left(\frac{\rho}{\overline{OD}}\right) + \arccos\left(\frac{\rho}{\overline{OA}}\right), \tag{31}$$

$$\overline{PA} = \sqrt{\overline{OD}^2 - \rho^2} - r_{\text{rou}} \rightarrow \overline{OA} = \sqrt{\overline{PA}^2 + \rho^2}. \tag{32}$$

The limits of variation of the parameters describing the involute section must now be modified with respect to those determined in Eq. (24). The minimum radius of involute will be defined by the length of the OA vector in Fig. 5:

$$\left(\overline{OA}\right)^2 - \left(r_{2x}^{R}\right)^2 - \left(r_{2y}^{R}\right)^2 = 0 \rightarrow u_{2\min}, \theta_{C2\min}. \tag{33}$$

Once these parameters are known, α is defined to be introduced in Eq. (31) as

$$\alpha = \arctan\left(\frac{r_{2x(u2\min)}^{R}}{r_{2y(u2\min)}^{R}}\right). \tag{34}$$

The variation limits of the θ_{R3} also change with the introduction of the tip rounding, and Eq. (25) is modified as

$$r_{2x(u2\min)}^{R} - r_{3x}^{R} = 0 \rightarrow \theta_{R3\min}. \tag{35}$$

This rounding arc will be taken into account for the contact force determination, both in terms of magnitude and direction.

3 Geometric Overlaps and Profile Modifications

The second step in the planetary modeling is the determination of the potential contact points and the geometric overlaps between profiles for a given position of the transmission. In a similar way as the profile definition, it is also possible to find the potential contact points and the geometric overlaps through analytical formulation. To this end, the contact over the line of action(LOA) is defined and the geometrical overlapping between profiles is determined for each potential contact point. This procedure is thoroughly described in[18]. Up to this point, all modelling processes have been based on the ideal involute profile,

with the addition of the tip rounding. In the real world, gears include profile modifications, which are designed to improve the dynamic behavior(e.g. smoothening the transmission error) and to reduce the stress levels in the system(avoiding for example the corner contact at the teeth tip). As the objective of this work is the study of these profile modifications in a planetary transmission, it is necessary to implement said modifications in the model.

As first assumption prior to the profile modification modeling, it can be stated that deviations in the profile shape do not affect the overall flexibility of the tooth nor the direction of contact. This means that profile modifications only alter the contact condition in terms of the magnitude of the geometric overlap, advancing or delaying the contact with respect to the non-modified case. Therefore, for the implementation of the profile modification, it is sufficient with the alteration of the geometric overlaps according to the quantity of profile relief.

Gear profile modifications are of diverse type, but generally they can be classified according to the section of the profile affected and the size of said modification. This way, there are tip and bottom relief, where material is removed respectively from the tooth tip and from zones near the root circumference. The depth of the modification as well as the length of the profile affected depend on the application: load level, contact ratio and other parameters of the transmission. For tip and bottom relief, and in the case of transmissions with a contact ratio between 1 and 2, modifications which affect only the multiple contact zone(two pair in contact for each mesh) are considered short, while if the effect is extended to the single contact zone, the modification is considered long. With respect to the modification shape, in this work only two cases are considered: linear and parabolic.

The modeling approach presented in this work is valid for the implementation of profile modifications in a planetary gear transmission, but it can also be used for the introduction of non-desired deviations in the profile, due for example to manufacturing errors. Both in the case of non-desired or deliberately designed modifications, the usual practice is to represent the magnitude of the deviation in a diagram with respect to the radius of curvature of the profile(distance s in Fig. 6). Thus, the correction $e(s)$ introduced(deviation of the actual profile with respect to the ideal profile) is defined by the maximum magnitude of the modification(C_T or C_B for the tip and bottom relief respectively), the length of the correction(ΔL_T or ΔL_B) and the shape of the modification: linear or parabolic. Positive values of correction means the removal of material and, therefore, a smaller radius of curvature s in the case of external gears, and a greater s in the case of internal gears, as shown in Fig. 7. The initial point of the relief from the pitch point P are marked with B and T for the base and tip, respectively, being possible to represent the relief as shown in Fig. 7.

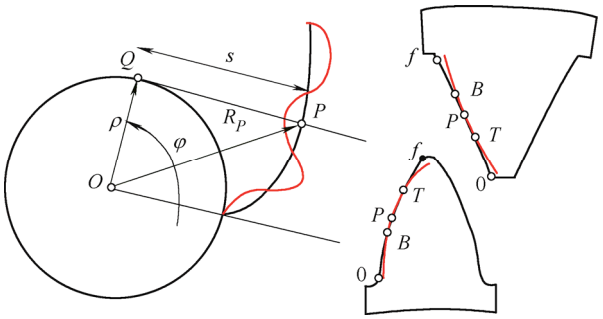

Fig. 6. Parameter definition for the profile modifications

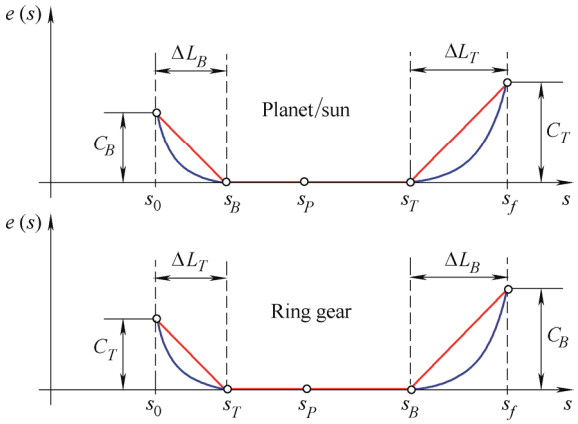

Fig. 7. Tip and base profile modification definition

The relief magnitude will be added to the geometrical overlap for each potential contact point, for the calculation of the contact forces. According to the definition of the profile modification, the relief will be as follows:

$$e_T^{\text{ext}}(s) = C_T \left(\frac{s - s_T}{\Delta L_T} \right)^n_{s \in [s_T, s_f]}, \tag{36}$$

$$e_T^{\text{int}}(s) = C_T \left(\frac{s - s_T}{\Delta L_T} \right)^n_{s \in [s_0, s_T]}, \tag{37}$$

$$e_B^{\text{ext}}(s) = C_B \left(\frac{s_B - s}{\Delta L_B} \right)^n_{s \in [s_0, s_B]}, \tag{38}$$

$$e_B^{\text{int}}(s) = C_B \left(\frac{s - s_B}{\Delta L_B} \right)^n_{s \in [s_B, s_f]}. \tag{39}$$

Eqs. (36) and (37) are used for tip relief in external (planet/sun) and inner gear (ring) respectively, Eqs. (38) and (39) for bottom relief. The modification shape is taken into account with the exponent n, 1 for linear and 2 for parabolic relief.

4 Meshing Forces and Dynamic Implementation

Next, a summary of the modeling approach used in this

work for the meshing forces calculation and the dynamic implementation is presented, being described with greater detail in Refs. [18–20]. The contact forces are computed in this model defining their relation with the deformations, which are obtained for a given position as the geometric overlaps between mating profiles. By solving a non-linear constrained system of equations, the contact forces cab thus be computed for a specific position. The relation between contact forces and deformations is obtained by using a modification of ANDERSSON's procedure[23]. The deformations are obtained as a combination of two terms: global and local. The structural term is due to linear deflections in the region far from the contact point, representing the deformation(shearing and bending) of the tooth and the whole gear body. On the other hand, the local term is used to describe the non-linear deformation near the region where the contact is taking place. Thus, the three problems described in Fig. 8 are combined, taking into account Saint-Venant theory for statically-equivalent loads: far away from the application point, differences among their effects can be neglected.

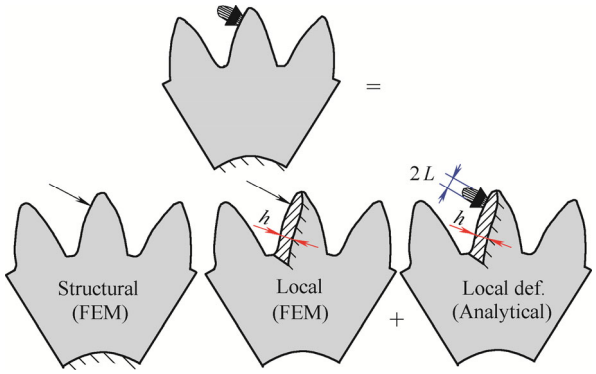

Fig. 8. Combination of structural and local deformations

Therefore, a boundary must be established at a distance h in order to consider both structural and local deformations. Structural deformations are then computed using Finite Element Method(FEM), with a unitary force applied on the potential contact point(Fig. 8 left). These deformations are valid only for regions far away from the contact point. Consequently, a correction is needed for regions closed to the contact point, where the deformation is going to be computed via Weber-Banashek formulation. Thus, a subtraction is applied near the contact point(depth $< h$), as it can be seen in Fig. 8(center). Total structural deformation is then obtained as a combination of the two first problems in Fig. 8(left and center).

Then, local deformation taking place at the region close to the contact point(Fig. 8 right) is computed by means of a non-linear analytical formulation, which is dependent on the depth h and length of contact zone L. Total deformation can be described as

$$\boldsymbol{u}_{Tj} = \boldsymbol{u}^{G1}_{\text{Local}}\left(f_j\right) + \boldsymbol{u}^{G2}_{\text{Local}}\left(f_j\right) + \boldsymbol{u}^{G1}_{\text{Struc},j}\left(f_{1:N}\right) + \boldsymbol{u}^{G2}_{\text{Struc},j}\left(f_{1:N}\right), \tag{40}$$

with the local non-linear analytical formulation defined as

$$u_{\text{Local}}(q) = \frac{2\left(1-\upsilon^2\right)}{\pi E}\frac{f}{b}\left[\ln\left(\frac{h}{L}+A\right) - \frac{\upsilon}{1-\upsilon}\left(\frac{h}{L}\right)^2(A-1)\right],$$

$$A = \sqrt{1+\left(\frac{h}{L}\right)^2}. \tag{41}$$

Computation of contact forces using this approach presents some advantages. Usually, the contact zone is two orders of magnitude smaller than teeth size. This means that using only FE models, a very fine mesh would be needed in the contact region. Also, as the contact zone changes during motion, a remesh would be needed for each position. With the hybrid approach used in this work, a much less fine mesh is accepted because it is only needed for computing structural deformations and no remesh is required. This reduces considerably the computational effort.

Regarding the dynamic implementation, a planar dynamic model of lumped masses is adopted in this work. The dynamic model must also include the dissipative phenomena, such as friction and damping. It is difficult to find in the literature a systematic modeling of these kind of efforts for gear transmissions, specially for its dynamic implementation. They can be classified by means of their dependency on losses by friction, rolling and deformation (dependent) and losses due to movement of fluid mass (independent). According to HÖHN[24], friction is the most important loss component if we compare it with rolling. Moreover, from the point of view of the system excitation, the importance of the friction force is even greater, not only because it acts out of the line of action, but because its direction change at the pitch point. In this work, friction forces and damping forces due to solid deformation and lubricant effect have been taken into account. Friction forces are implemented using a Coulomb model, where the contact forces are multiplied by the friction coefficient. The definition of the friction coefficient takes into account its zero value at the pitch point, but also lubricant effects, such as sliding velocity, viscosity, load amplitude and rugosity. The whole model has been implemented in MATLAB® and the dynamic part integrated in SIMULINK®. Further details on these modeling aspects can be found in Refs. [18–20].

5 Profile Modification and Results

The goal of the work is the application of the planetary model to the design of a profile modification set for the three gears of the planetary. A real transmission has been selected for its simulation, whose parameters are shown in Table 1.

Table 1. Transmission parameters

Parameter	Sun	Planet	Ring
No. of teeth	16	24	65
Modulus m/mm	4.23	4.23	4.23
Width/mm	25	25	25
Pressure angle (°)	25	25	25
Tool addendum/mm	1.35m	1.35m	–
Tool deddendum/mm	1.15m	1.25m	–
Tool tip/mm	0.05m	0.05m	–
Teeth tip round/mm	0.05m	0.05m	0.05m
Axis radius/mm	20	20	156.4
Elastic modulus/GPa		207	
Poisson coefficient		0.3	

The relief parameters have been designed based on the levelling of the load sharing ratio, which has already been defined as the individual portion of the load that each planet carries with respect to the total transmitted load. The profile modifications are closely related with the LSR characteristics. The profile modifications allow for the avoidance of corner contact, which as already has been stated is one of the main sources of uneven load sharing for planetary systems with a floating central member. Thus, the LSR levels with the introduction of the modifications, due to the elimination of contacts out of the line of action.

In the example case, the modification values have been varied until certain threshold of improvement in the LSR is achieved. In Fig. 9 are shown the results for the original LSR(without modification) and for the final selection of modification parameters.

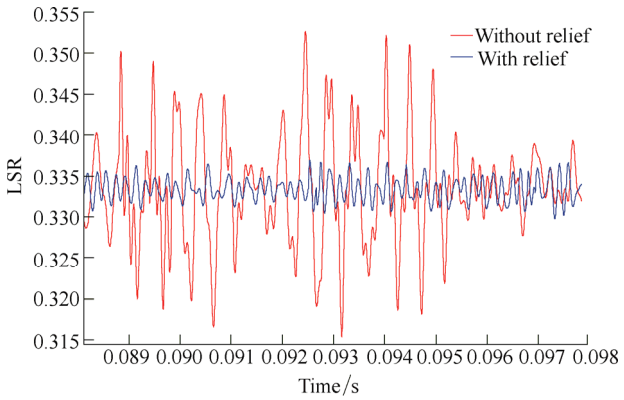

Fig. 9. Dynamic LSR

The design of the modification is based on a tip linear relief for every gear, and the resulting modification parameters (according to the definition presented in Section 3) were C_T=0.014 mm for both external gears and C_T=0.010 mm for the ring. The profile modification length to which the correction is applied is ΔL_T=3 mm for the planet, ΔL_T=2.5 mm for the sun and ΔL_T=4 mm for the ring.

As the design of the profile modification set is based on the improvement on the LSR, is evident that this characteristic is implicitly better in the modified case. Nevertheless, some other dynamic characteristics can be studied to verify if the behavior improvement is general.

As for the transmission error, which is one of the most typical transmission characteristics used for the assessment of the dynamic behavior, in Fig. 10 is presented for both cases(modified and unmodified).

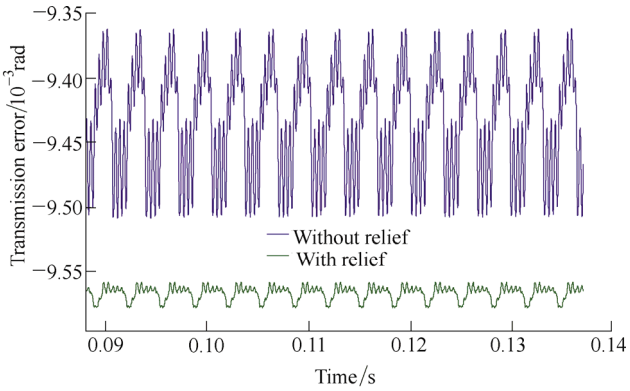

Fig. 10. Overall planetary transmission error(sun)

The mean value of the transmission error is increased when relief is included, although this has only a slight effect on the dynamic characteristics. One of the reason for the increase in the TE is the reduction of the overall stiffness of the planetary, being the single contact periods for each mesh in play prolonged. As a second and more important factor, the TE is a characteristic with a pure kinematic component, and the fact that the relief reaches the primitive point for each mesh implies an extra free rotation of the wheels to achieve contact. The peak-to-peak variation of the TE is significantly reduced, due to the less abrupt change in the number of pairs in contact, with a much smoother transition.

In Fig. 11 the orbit of the sun is presented for the modified and unmodified cases. Again, it is possible to appreciate the improvement in terms of orbit radius reduction when the involute profiles include relief.

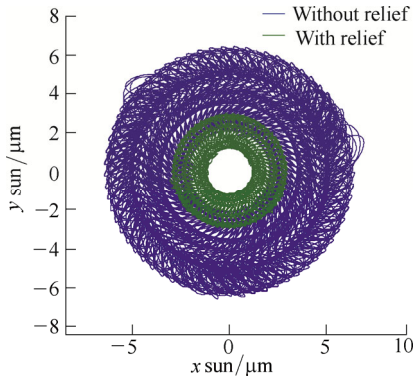

Fig. 11. Sun orbit

As additional demonstration of the model capabilities and relief improvement, the vertical force transmitted through the ring to the support is shown in Fig. 12. There is a considerable reduction of the force when the relief is introduced. The main factor that determines this reduction is the improvement of the load sharing ratio. When the LSR is uneven, the symmetry of the 3-planet system is broken and the support forces skyrocket.

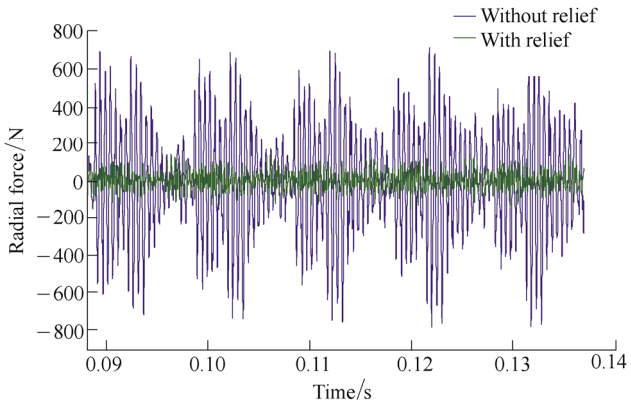

Fig. 12. Dynamic vertical force in the ring

6 Conclusions

A planetary gear model for the design of profile modifications is been presented, with the description focused on the profile geometry definition. The approach allows for the realistic reproduction of the cutting process of external and internal gears:

(1)This method takes into account the undercutting of the teeth, also directly defining the hypotrochoid section that connects the involute profile and the root circumference.

(2)To avoid the corner contact at the teeth tip, a rounding arc is added, which allows to calculate the meshing forces in magnitude and direction for the entire contact period, including during these out of line contacts.

(3) The procedure for the modeling of profile deviations can be used for the introduction of both manufacturing errors and designed profile modifications.

(4) The modeling approach allows for the possibility of linear and parabolic correction, with any size and length of both tip and bottom classes relief.

(5) The correction effect on the tooth flexibility is neglected, which allows for the easy implementation of the profile deviation as a simple geometric reduction in the geometric overlap between mating profiles for a given position of the transmission.

A set of reliefs is designed for the minimization of the load sharing ratio. The modification adopted is linear, C_T=0.014 mm for both external gears and C_T=0.010 mm for the ring, with length of ΔL_T=3 mm for the planet, ΔL_T=2.5 mm for the sun and ΔL_T=4 mm for the ring. The relief is designed for obtaining a leveling in the LSR, eliminating the contacts out of the line of action. As additional results, it has been found that with the modifications:

(1) The sun orbit radius experiments a significant reduction of almost 60%.

(2) The mean value of the TE is increased when modifications are included, but there is a great reduction in the peak-to-peak variation of the TE, due to the smoother transition between changes in the number of contacting pairs.

The vertical force transmitted through the ring to the support is greatly reduced when the relief is introduced. The force symmetry is maintained through the meshing period, and the contact forces cancel each other, consequently reducing the force transmitted to the support.

References

[1] SMITH J D. *Gear noise and vibration*[M]. Cambridge: Marcel Dekker Inc., 1999.

[2] HENG A, ZHANG S, TAN A, et al. Rotating machinery prognostics: State of the art, challenges and opportunities[J]. *Mechanical Systems and Signal Processing*, 2009, 23(3): 724–739.

[3] HAYASHI T, LI Y, HAYASHI I, et al. Measurement and some discussions on dynamic load sharing in planetary gears[J]. *Bulletin of the JSME*, 1986, 29(253): 2290–2297.

[4] HIDAKA T, TERAUCHI Y. Dynamic behavior of planetary gear - 1st report, load distributions in planetary gear[J]. *Bulletin of the JSME*, 1976, 19(132): 690–698.

[5] SINGH A. Load sharing behavior in epicyclic gears: Physical explanation and generalized formulation[J]. *Mechanism and Machine Theory*, 2010, 45(3): 511–530.

[6] ABOULEISMAN V, VELEX P, BECQUERELLE S. Modeling of spur and helical gear planetary drives with flexible ring gears and planet carriers[J]. *Journal of Mechanical Design*, 2007, 129: 95–106.

[7] PALMER W, FUEHRER R. Noise control in planetary transmissions[J]. *SAE Technical Paper No. 770561*, 1977.

[8] ABOULEISMAN V, VELEX, P. A hybrid 3D finite element/lumped parameter model for quasi-static and dynamic analyses of planetary/ epicyclic gear sets[J]. *Mechanism and Machine Theory*, 2006, 41(6): 725–748.

[9] INALPOLAT M, KAHRAMAN A. A dynamic model to predict modulation sidebands of a planetary gear set having manufacturing errors[J]. *Journal of Sound and Vibration*, 2010, 329(4): 371–393.

[10] AL-SHYYAB A, KAHRAMAN A. A non-linear dynamic model for planetary gear sets[J]. *Proceedings of the Institution of Mechanical Engineers, Part K*, 2007, 221(4): 567–576.

[11] BAHK C J, PARKER R G. Analytical investigation of tooth profile modification effects on planetary gear dynamics[J]. *Mechanism and Machine Theory*, 2013, 70: 298–319.

[12] SEAGER D L. Conditions for the neutralization of excitation by the teeth in epicyclic gearing[J]. *Proceedings of Institution of Mechanical Engineers*, 1975, 17(5): 293–298.

[13] INALPOLAT M, KAHRAMAN A. A dynamic model to predict modulation sidebands of a planetary gear set having manufacturing errors[J]. *Journal of Sound and Vibration*, 2010, 329(4): 371–393.

[14] LIU G, PARKER R G. Dynamic modeling and analysis of tooth profile modification for multimesh gear vibration[J]. *ASME Journal of Mechanical Design*, 2008, 130(12): 121402-1–121402-13.

[15] VELEX P, FLAMAND L. Dynamic response of planetary trains to mesh parametric excitations[J]. *ASME Journal of Mechanical Design*, 1996, 118(1): 7–14.

[16] LIN J, PARKER R G. Planetary gear parametric instability caused by mesh stiffness variation[J]. *Journal of Sound and Vibration*, 2002, 249(1): 129–145.

[17] PARKER R G, AGASHE V, VIJAYAKAR S M. Dynamic response of a planetary gear system using a finite element/contact mechanics model[J]. *ASME Journal of Mechanical Design*, 2000, 122(3): 304–310.

[18] FERNANDEZ DEL RINCON A, VIADERO F, et al. A model for the study of meshing stiffness in spur gear transmissions[J]. *Mechanism and Machine Theory*, 2013, 61: 30–58.

[19] FERNANDEZ A, IGLESIAS M, DE-JUAN A, et al. Gear transmission dynamic: Effects of tooth profile deviations and support flexibility[J]. *Applied Acoustics*, 2014, 77: 138–149.

[20] FERNANDEZ DEL RINCON A. *An advanced model for the study of the vibratory behavior of gear transmission systems*[D]. Santander: University of Cantabria, 2010.
[21] LITVIN F L, FUENTES A. *Gear geometry and applied theory*[M]. 2nd ed. Cambridg: Cambridge University Press, 2004.
[22] VEDMAR L. *On the design of external involute helical gears, Transactions of machine elements division*[M]. Lund: Lund Technical University, 1981.
[23] ANDERSSON A, VEDMAR L. A dynamic model to determine vibrations in involute helical gears[J]. *Journal of Sound and Vibration*, 2003, 260(2): 195–212.
[24] HÖNH B. Improvements on noise reduction and efficiency of gears[J]. *Meccanica*, 2010, 45(3): 425–37.

Biographical notes

IGLESIAS Miguel is a research professor and received his PhD degree at *University of Cantabria, Spain* in 2013. His research activities are focused on machinery condition monitoring and gear dynamic modelling.
E-mail: iglesiassm@unican.es

FERNÁNDEZ DEL RINCÓN Alfonso is an associate professor and a PhD candidate supervisor at *University of Cantabria, Spain*. He received his PhD degree from *University of Cantabria, Spain* in 2010. His research interests include rotordynamics and machinery condition monitoring.
E-mail: fernandra@unican.es

DE-JUAN Ana Magdalena is an assistant professor at *University of Cantabria, Spain*. She received her PhD degree from *University of Cantabria, Spain* in 2011. Her research interests fall in the kinematics synthesis and multibody modeling.
E-mail: dejuanam@unican.es

GARCIA Pablo is currently an associate professor at *Mechanical Engineering Research Group, University of Cantabria, Spain*. His main research activities include kinematics synthesis, machine dynamics and NVH assessment.
E-mail: garciapf@unican.es

DIEZ Alberto is an engineer and an assistant lecturer at *University of Cantabria, Spain*, and is a PhD candidate in the field of gear efficiency modeling. He received his master degree on industrial engineering in 2011.
E-mail: diezia@unican.es

VIADERO Fernando is a full professor and the head at the *Mechanical Engineering Research Group, University of Cantabria, Spain*. He received his PhD degree from *Faculty of Engineering of Bilbao, Spain*, in 1984. His research interests include dynamics of gear transmissions, analysis and synthesis of mechanisms, and vehicle suspension design.
Tel: +34-942201854; E-mail: viaderof@unican.es